SI for

Synthesis of liquid fuel via direct hydrogenation of CO_2

Zhenhong He, Meng Cui, Qingli Qian, Jingjing Zhang, Huizhen Liu, Buxing Han

This PDF file includes:

www.pnas.org/cgi/doi/10.1073/pnas.1821231116

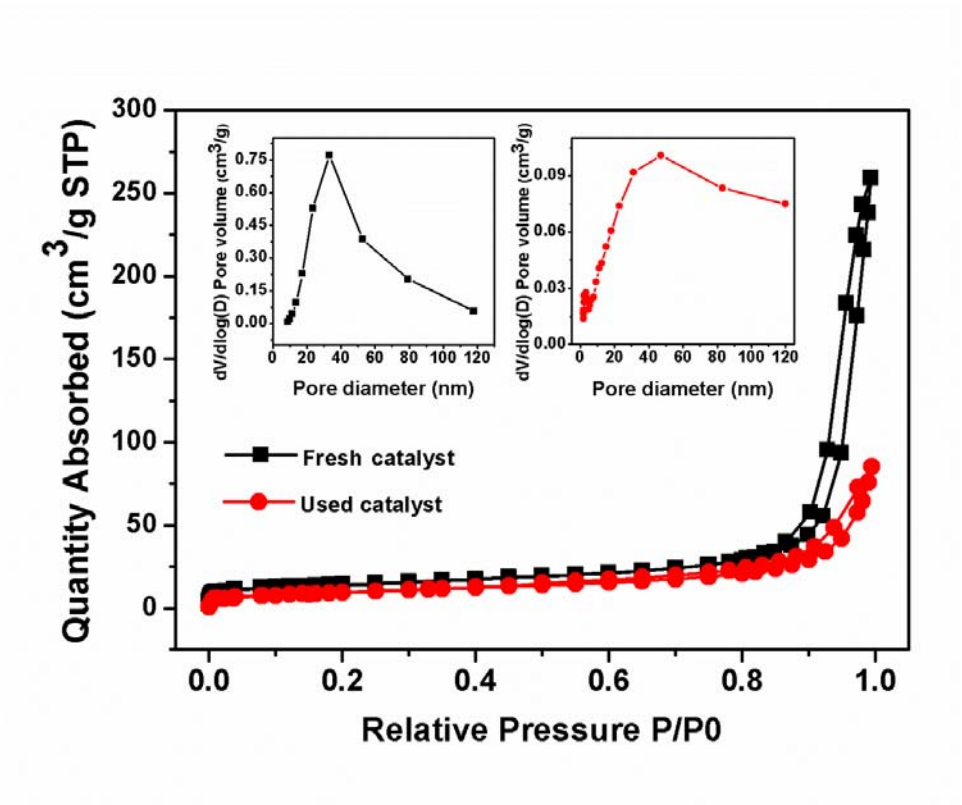

Fig. S1. The N_2 adsorption isotherm and pore diameter distribution (inset) of Co_6/MnO_x.

Note: The BET surface areas of the fresh catalyst and the used catalyst were 49.4 and 34.4 m^2/g, respectively.

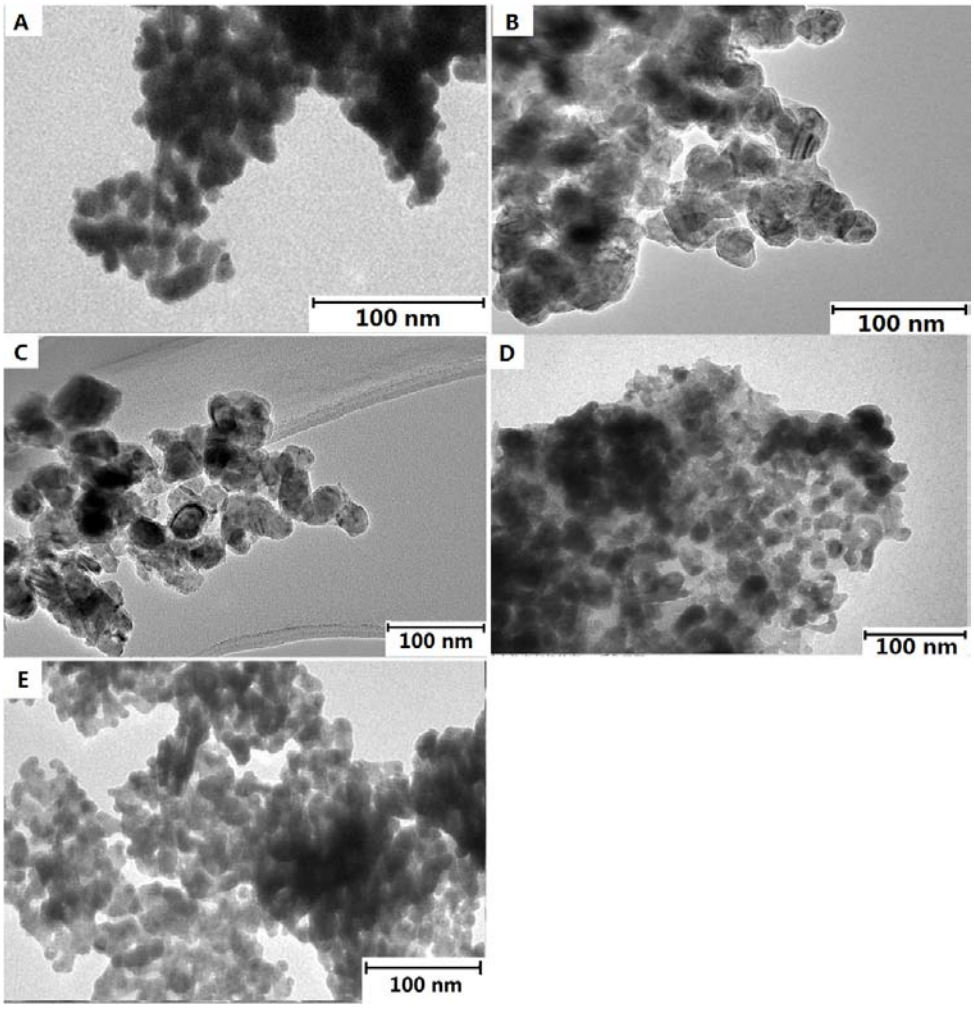

Fig. S2. The TEM images of Co^0 (A), Co_2/MnO_x (B), Co_6/MnO_x (C), Co_{10}/MnO_x (D) and Co_{14}/MnO_x (E).

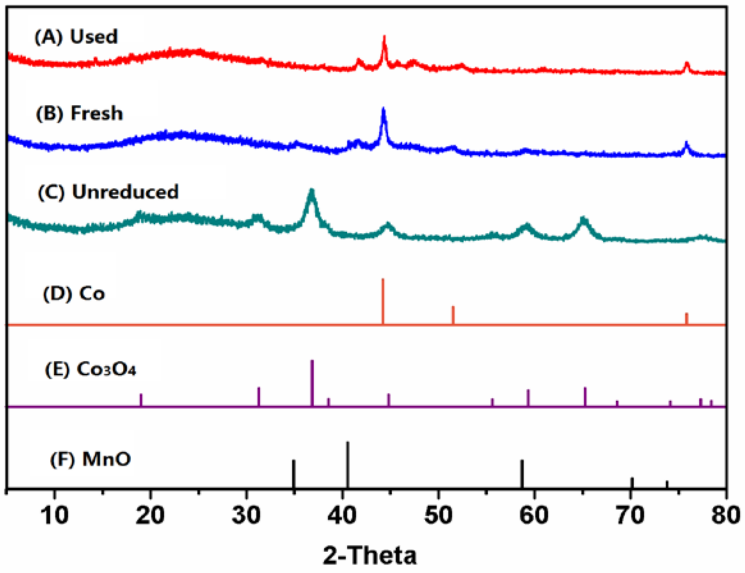

Fig. S3. XRD patterns of Co_6/MnO_x: (A) the catalyst after four cycles, (B) fresh catalyst, (C) unreduced catalyst, (D) JCPDF Card No.15-0806, Co, (E) JCPDF Card No.43-1003, Co_3O_4, (F) JCPDF Card No. 07-0230, MnO.

Note: The unreduced catalyst precursor exhibited a Co_3O_4 structure (C vs. E). The peaks appeared at 19.1°, 31.4°, 36.9 °, 38.6°, 44.9°, 55.7°, 59.4°, 65.2°, 73.7°, and 77.3° can be indexed to the (111), (220), (311), (222), (400), (422), (511), (440), (620), and (533) planes of Co_3O_4 (JCPDF Card No. 43-1003), respectively. After reduction by H_2 at 400 °C for 1 h, the Co^0 and MnO crystallites in the catalyst appeared (B *vs.* D and F). The peaks appeared at 35.1°, 40.7°, and 58.8° can be assigned to (111), (200), and (220) planes of MnO (JCPDF Card No.07-0230), respectively. The other peaks appeared at 44.2°, 51.5°, and 75.8° are attributed to (111), (200), and (220) of Co^0 species (JCPDF Card No.15-0806), respectively.

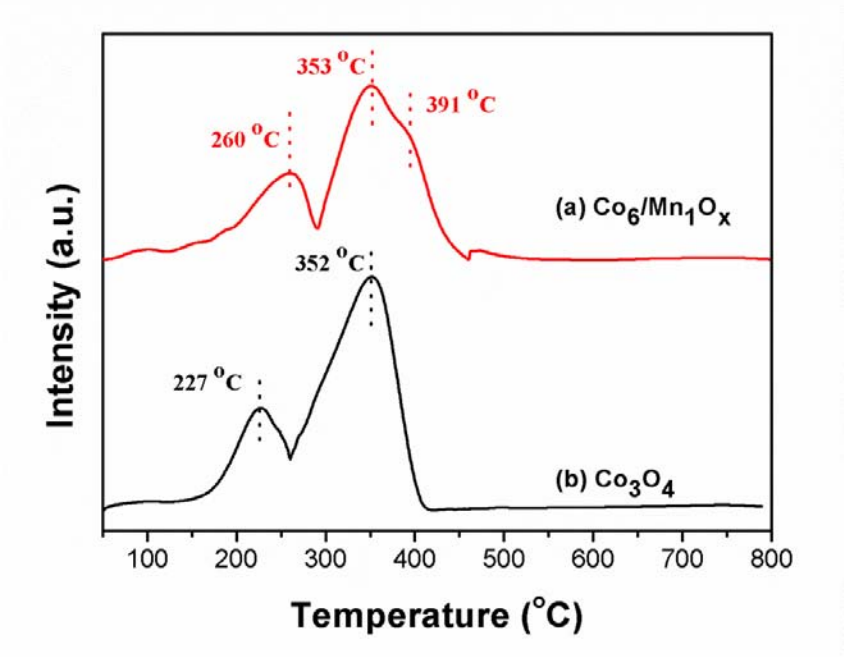

Fig. S4. TPR spectra of the unreduced Co_6/MnO_x (A) and the commercial Co_3O_4 (B).

Note: In the H_2-TPR spectra of Co_3O_4, two peaks at 227 °C and 352 °C can be assigned to the reduction peaks of Co_2O_3 to CoO and CoO to Co^0, respectively. However, in the TPR profile of unreduced Co_6/MnO_x, the first peak appeared at 260 °C was the reduction of Co_2O_3 to CoO, which was higher than that of the pure Co_3O_4 catalyst. The subsequent peaks appeared at 353 and 391 °C were the overlapped peaks of reduction of CoO to Co and the partial reduction of Mn_2O_3 to Mn_3O_4 *(1)*. The TPR results indicated that the Mn could retard the reduction of Co_3O_4, demonstrating that strong interaction existed between Co and Mn species.

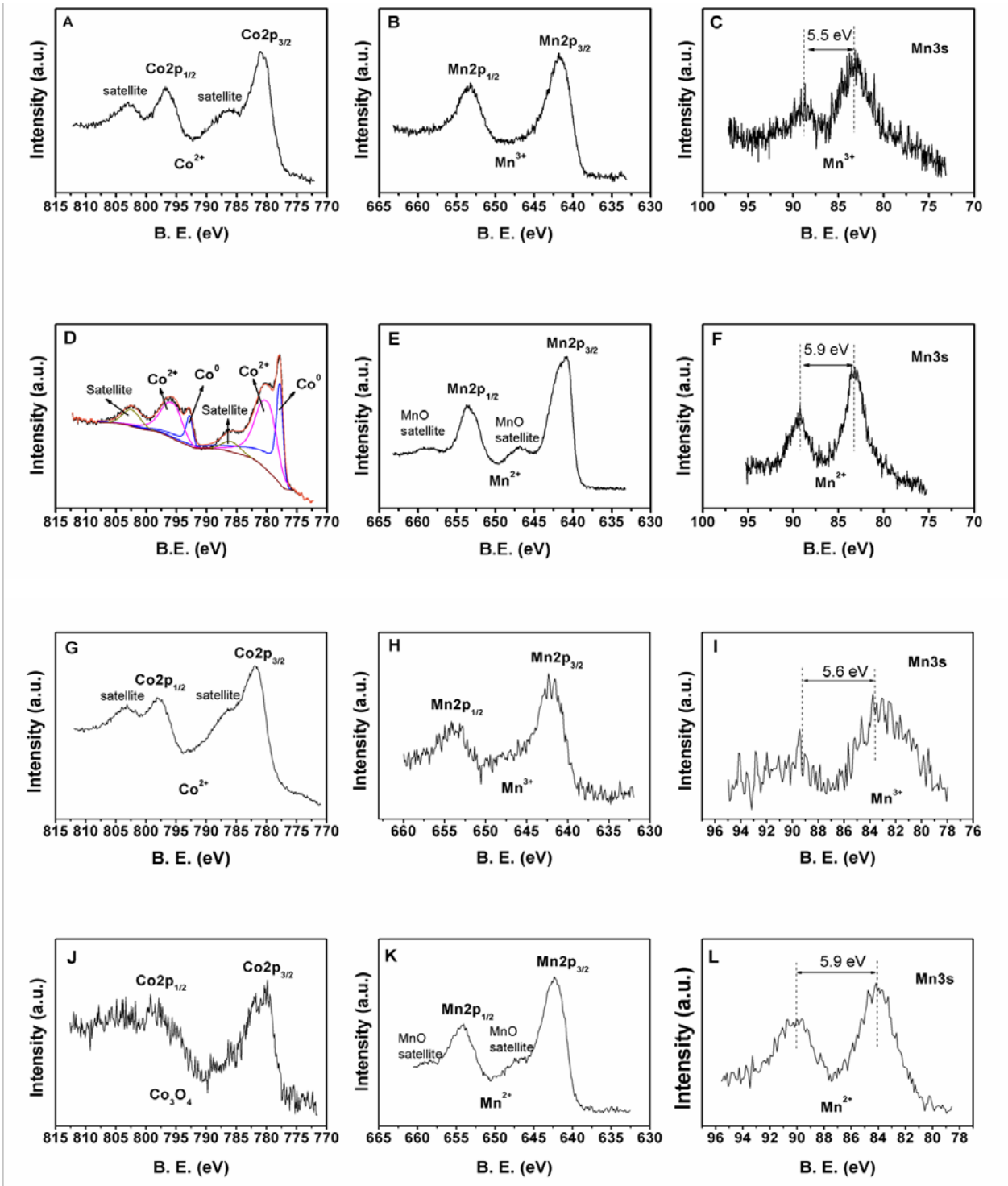

Fig. S5. XPS spectra of Co_6/MnO_x: Co2p (A), Mn2p (B) and Mn3s (C) of the fresh catalyst; Co2p (D), Mn2p (E) and Mn3s (F) of the catalyst under semi in situ characterization after treatment with H_2 at 200 ^oC for 2 h; Co2p (G), Mn2p (H) and Mn3s (I) of the catalyst after CO_2 hydrogenation; Co2p (J), Mn2p (K) and Mn3s (L) of the catalyst after CO hydrogenation.

Note: In the XPS spectra of the fresh catalyst, the surface Co atoms were all Co^{2+} (fig. S5A). The peaks at 780.8 eV and 796.5 eV are assigned to Co^{2+} $2p_{3/2}$ and Co^{2+} $2p_{1/2}$, respectively, and the peaks appeared at 786.5 eV and 802.9 eV are their corresponding shake-up satellites *(2)*. The surface Mn atoms of the fresh catalyst were all Mn^{3+}. The peaks at 641.7 eV and 653.3 eV can be ascribed to Mn^{3+} $2p_{3/2}$ and Mn^{3+} $2p_{1/2}$, respectively (fig. S5B). The Mn3s spectrum also helped to determine the valence of the Mn atom (fig. S5C). The distance between the two peaks of Mn3s was 5.5 eV, which agreed well with that of the Mn^{3+} *(3)*. In the spectra of the semi in situ characterization, the surface Co atoms had two valences, i.e., Co^0 and Co^{2+} (fig. S5D). The peaks at 777.9 eV and 792.9 eV are ascribed to Co^0 $2p_{3/2}$ and Co^0 $2p_{1/2}$, respectively *(4)*. The peaks around 780.5 eV and 796.0 eV are assigned to Co^{2+} $2p_{3/2}$ and Co^{2+} $2p_{1/2}$, respectively, and the peaks at 786.2 eV and 802.6 eV were their corresponding shake-up satellites. The Mn atoms were reduced to Mn^{2+} by H_2. The peaks at 641.1 eV and 653.6 eV were attributed to Mn^{2+} $2p_{3/2}$ and Mn^{2+} $2p_{1/2}$, respectively, and the peaks around 646.9 eV and 658.8 eV were their corresponding satellites (fig. S5E). The distance between two peaks of Mn1s was 5.9 eV, which coincided well with that of the Mn^{2+} (fig. S5F). The spectra of the catalyst after CO_2 hydrogenation were shown in fig. S5G-I. The results indicated that they were similar to those of the fresh catalyst (fig. S5A-C). After CO hydrogenation, the atomic% of the elements on catalyst surface (C 63.03%, O 30.86%, Mn 5.15%, Co 0.96%) revealed that most of the Co atoms on the catalyst surface could be coated by carbon deposit. Accordingly, the signal of Co was very weak. In the spectra of the catalyst after CO hydrogenation, the peak at 780.6 eV could be assigned to Co $2p_{3/2}$ of Co_3O_4 (fig. S5J). From the satellites of the Mn 2p (fig. S5K) and the distance between the two peaks of the Mn3s (fig. S5L), we can deduce that the Mn element on the surface of the catalyst after CO hydrogenation was Mn^{2+}.

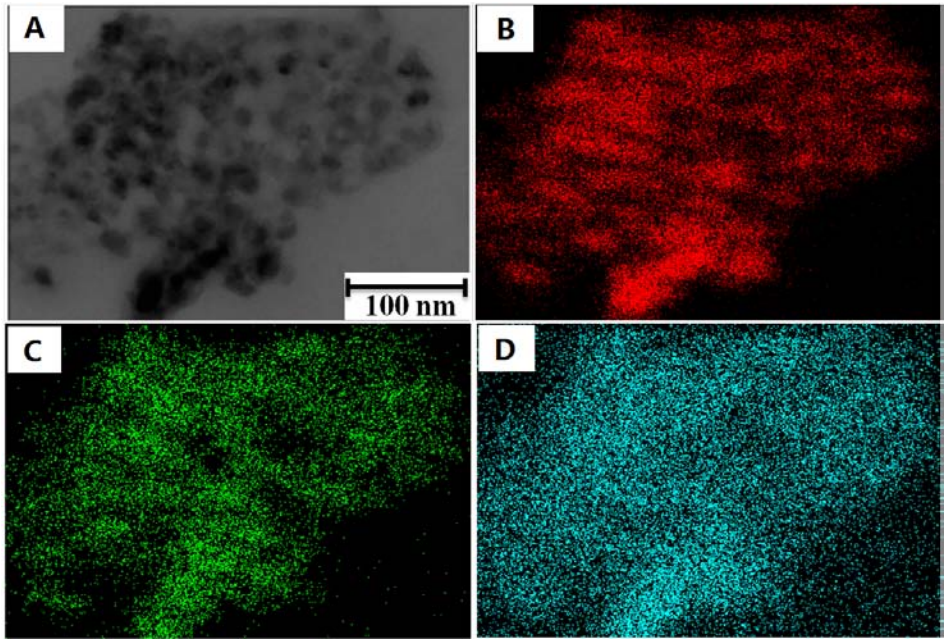

Fig. S6. The TEM image (A) and corresponding EDS elemental mapping (B, Co; C, Mn; D, O) of Co_6/MnO_x.

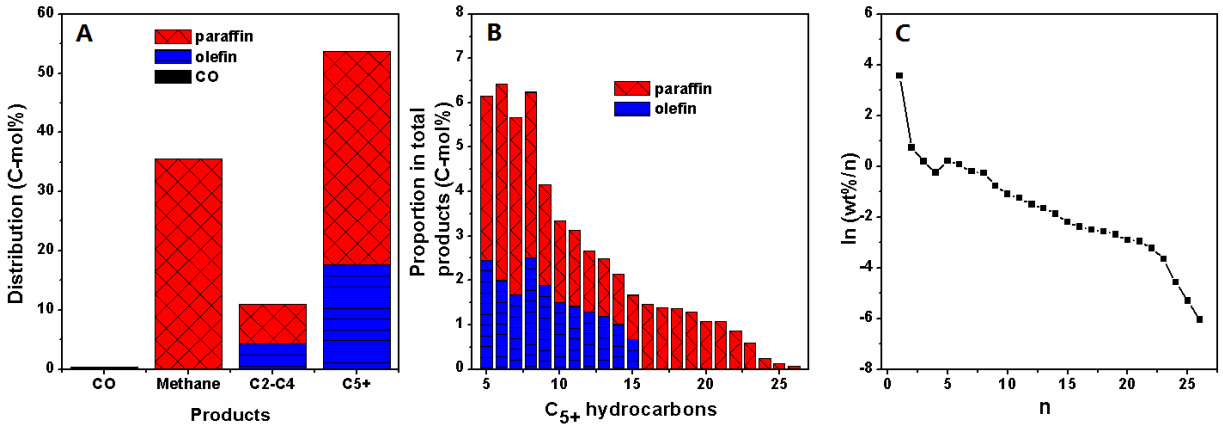

Fig. S7. The detailed hydrocarbon distribution and the Anderson-Schulz-Flory plot of the reaction product in entry 1 of Table 1. The hydrocarbons consisted of n-paraffins and minor linear monoolefins. The selectivity of paraffins in the total hydrocarbons was 78.1 C-mol%, and the selectivity of paraffin in the C_{5+} products was 67.2 C-mol%.

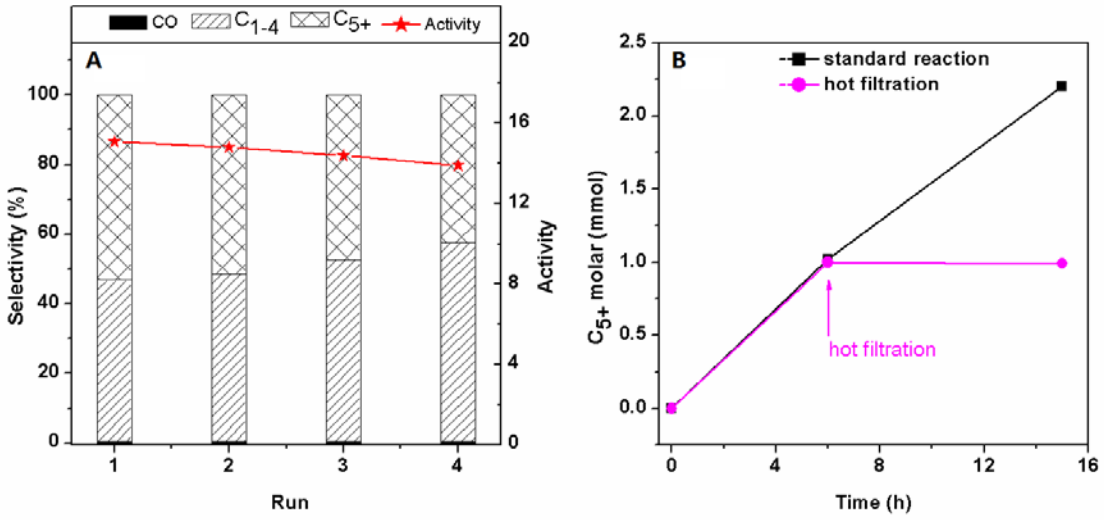

Fig. S8. The results of recycling test of the catalyst (A) and hot filtration test (B). The condition was the same as that of entry 1 in Table 1.

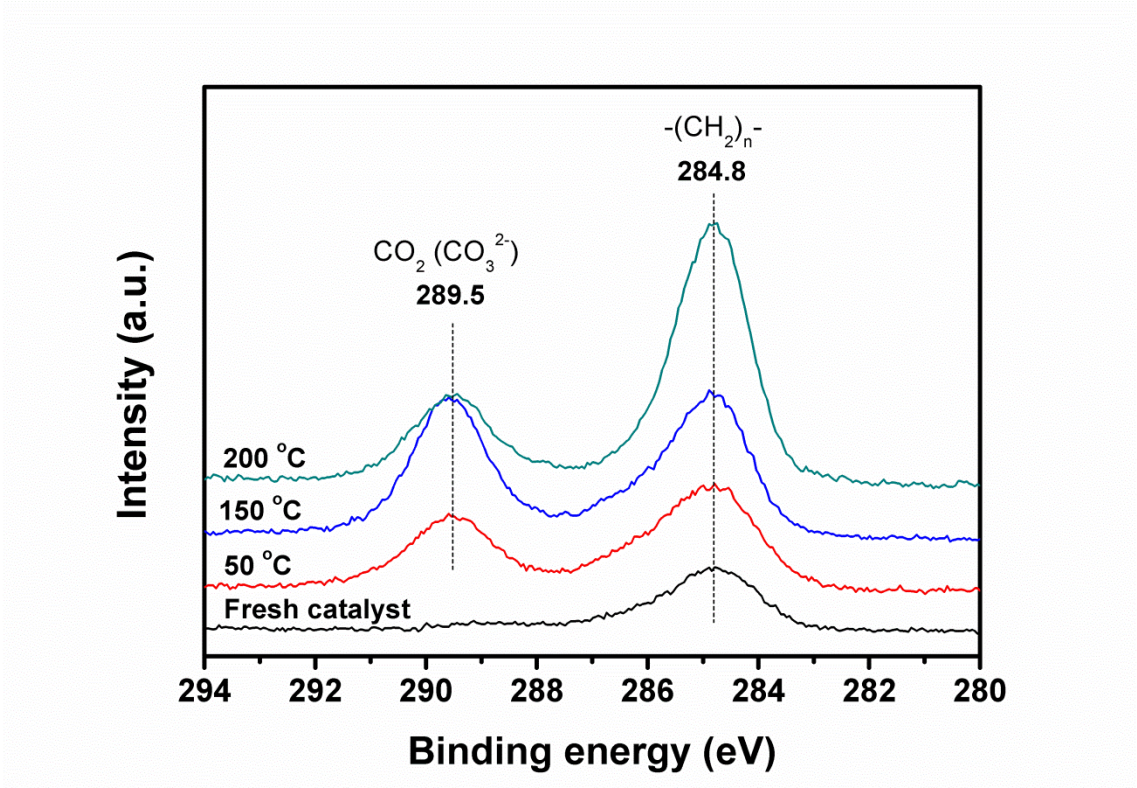

Fig. S9. Semi in situ XPS analysis of Co_6/MnO_x after CO_2 adsorption at different temperatures. The catalyst was pretreated with H_2 at 200 ^oC for 2 h before the adsorption test.

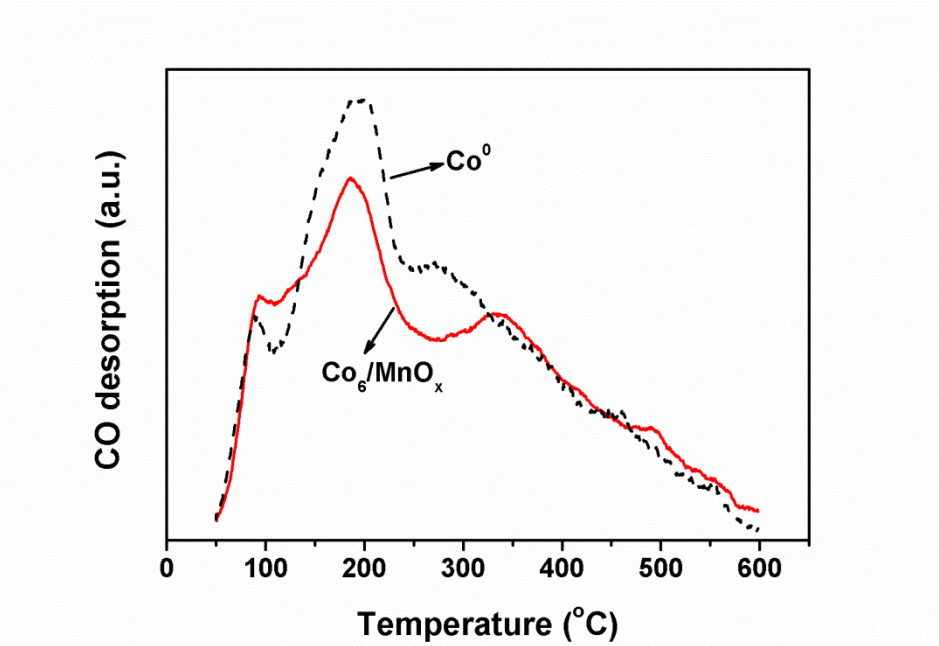

Fig. S10. The CO-TPD data of Co_6/MnO_x and Co^0. The TPD signals have been normalized to the mass of the tested samples.

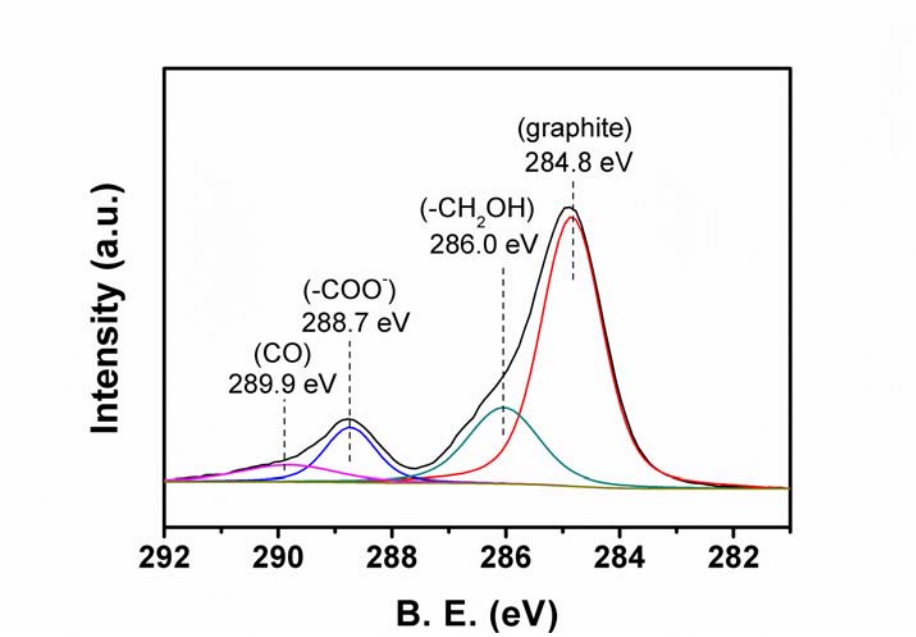

Fig. S11. The XPS spectra (C1s) of Co_6/MnO_x after CO hydrogenation.

Note: After CO hydrogenation, the atomic% of the elements on catalyst surface (C 63.03%, O 30.86%, Mn 5.15%, Co 0.96%) revealed that most of the Co atoms on the catalyst surface were coated by carbon deposit. Accordingly, the XPS signal of Co was very weak. As is shown in table S2, the catalytic performance of CO hydrogenation was very poor and little long chain hydrocarbon was produced in the reaction. Hence the peak at 284.8 eV should be ascribed to graphite. This fact is consistent with the pathway of the FTS, where CO firstly dissociates in to C and O atoms on the catalyst surface (*Ref. 22 of the article*). Furthermore, addition of Mn to Co based catalyst may also accelerate the dissociation and disproportionation of CO (*Ref. 21 of the article*). However, the carbon deposit could not be further converted because the Mn promoter inhibited the adsorption of H_2 on the catalyst surface.

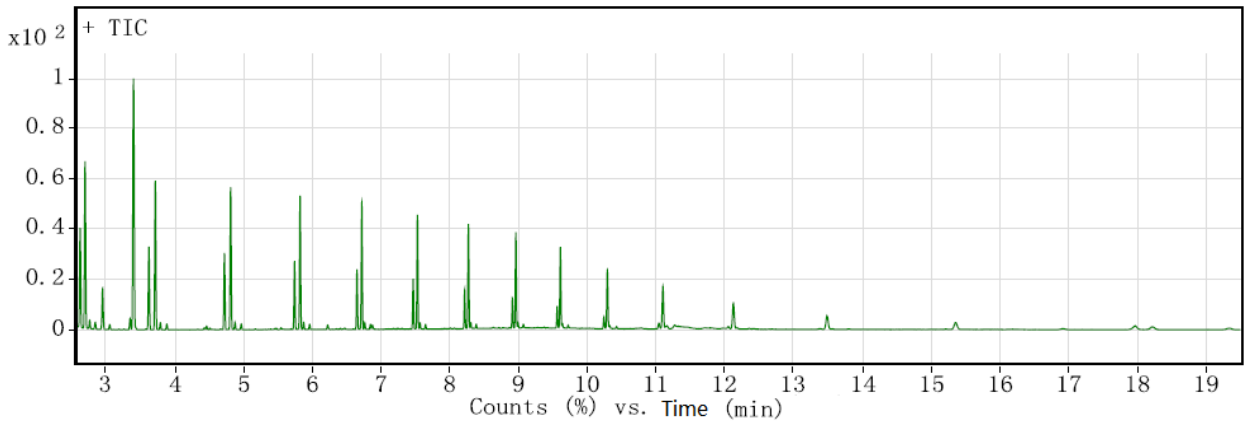
x10 2
+ TIC
1
0.8
0.6
0.4
0.2
0
3 4 5 6 7 8 9 10 11 12 13 14 15 16 17 18 19
Counts (%) vs. Time (min)

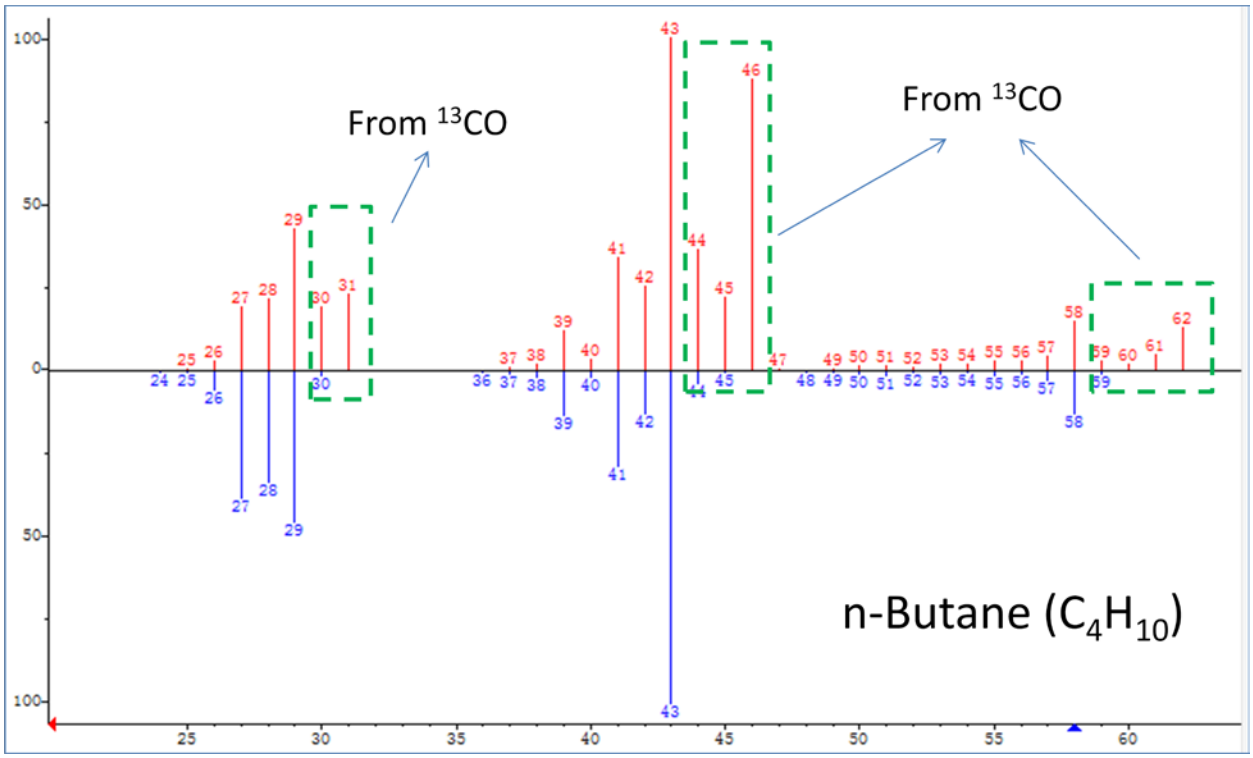
From ^{13}CO
From ^{13}CO
n-Butane (C_4H_{10})
100
50
0
50
100
25 30 35 40 45 50 55 60

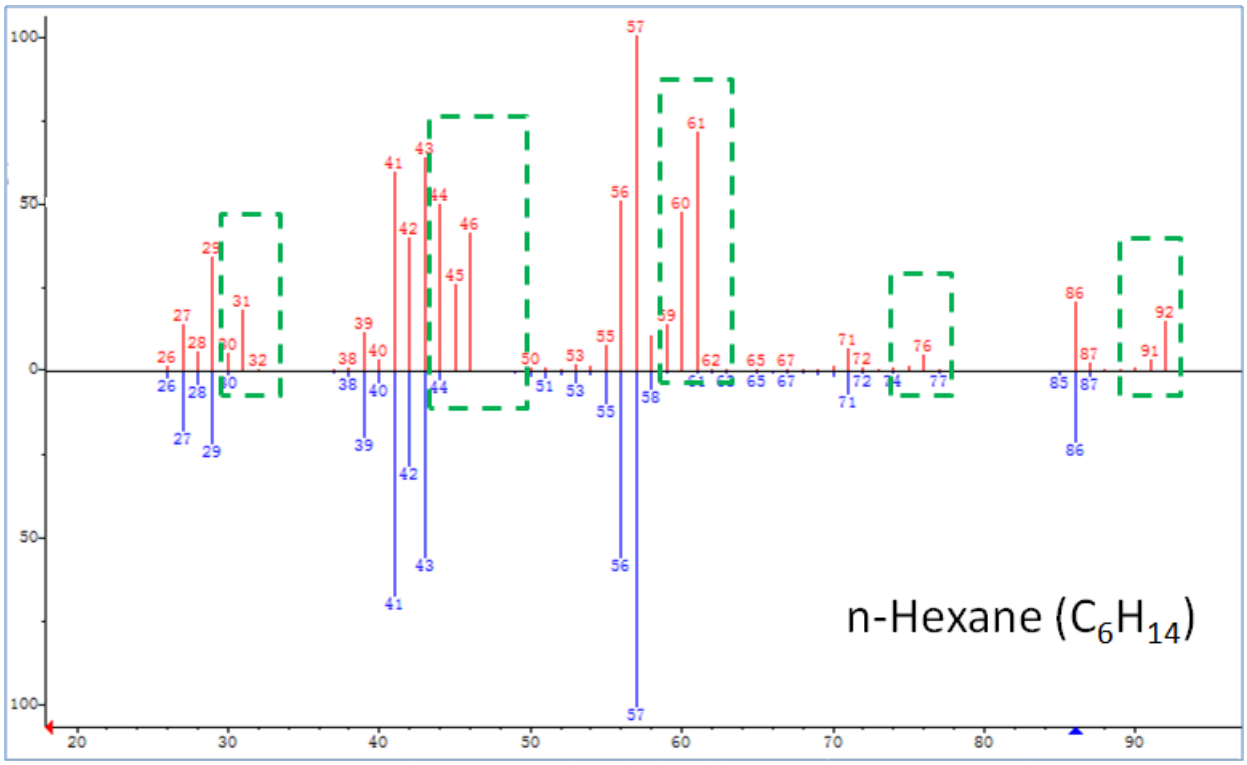
n-Hexane (C_6H_{14})

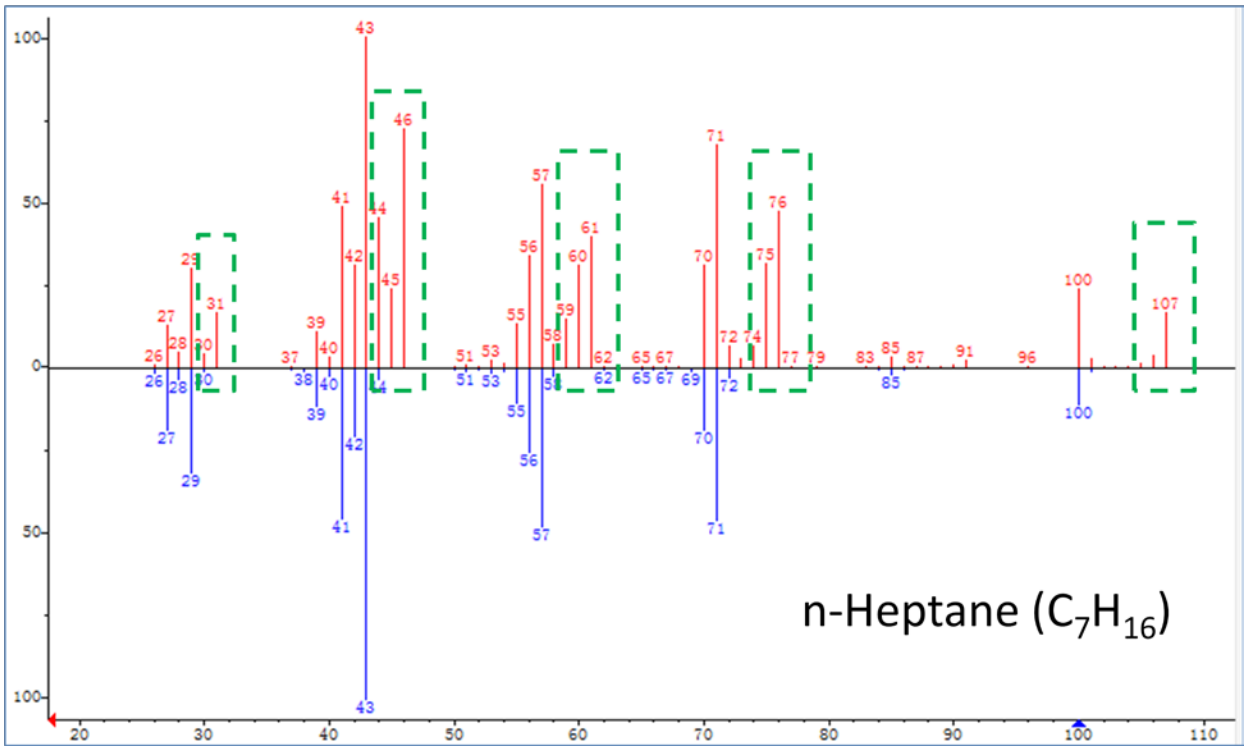
n-Heptane (C_7H_{16})

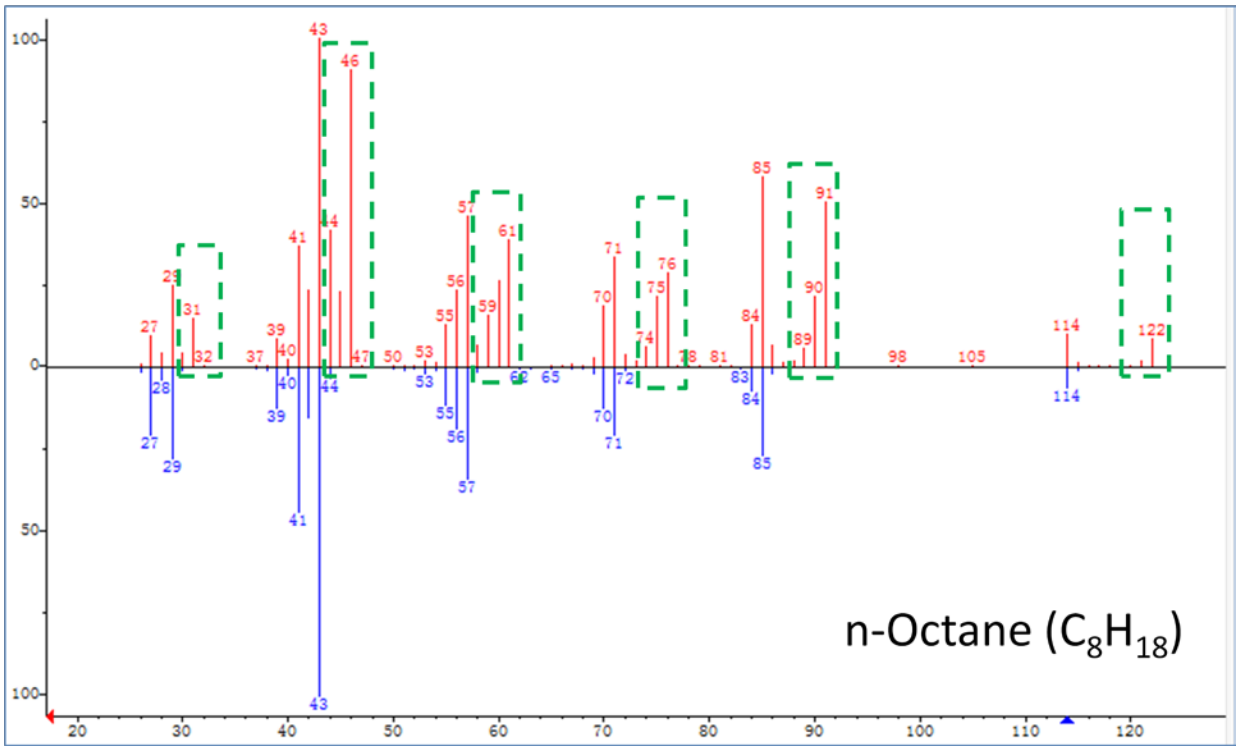
n-Octane (C_8H_{18})

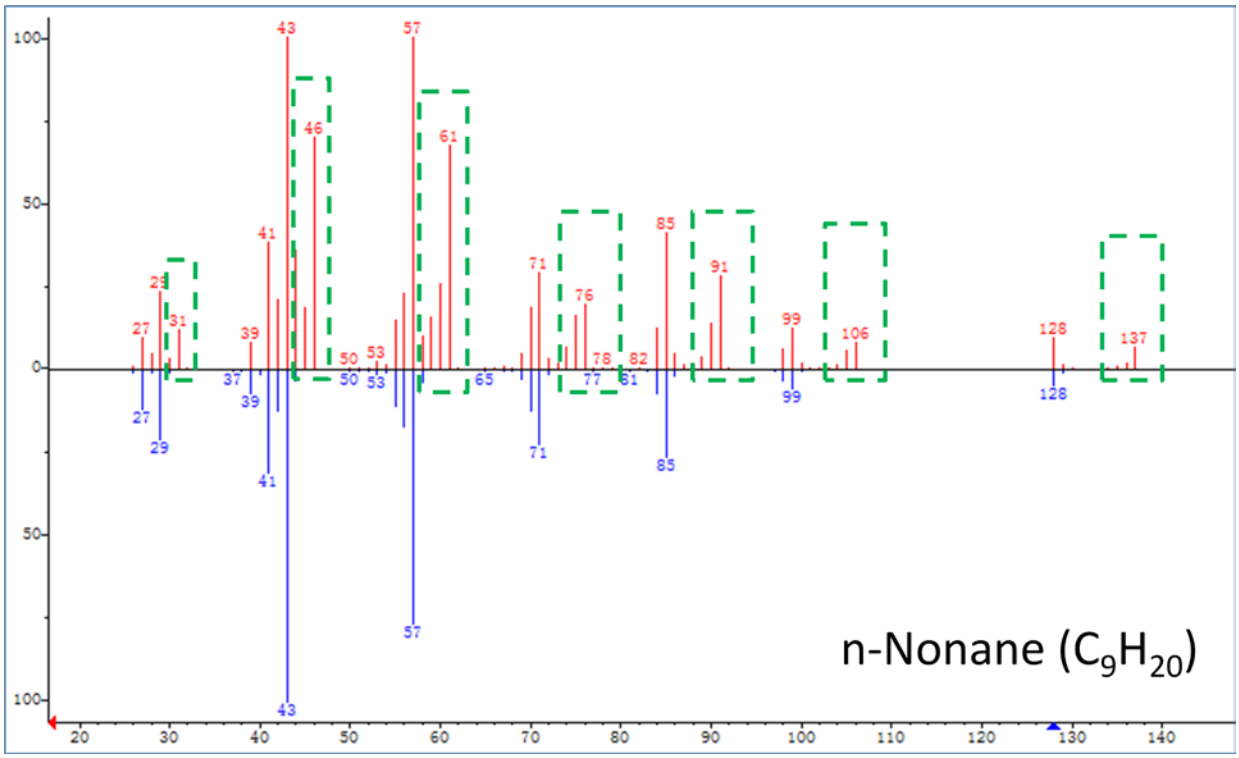
n-Nonane (C_9H_{20})

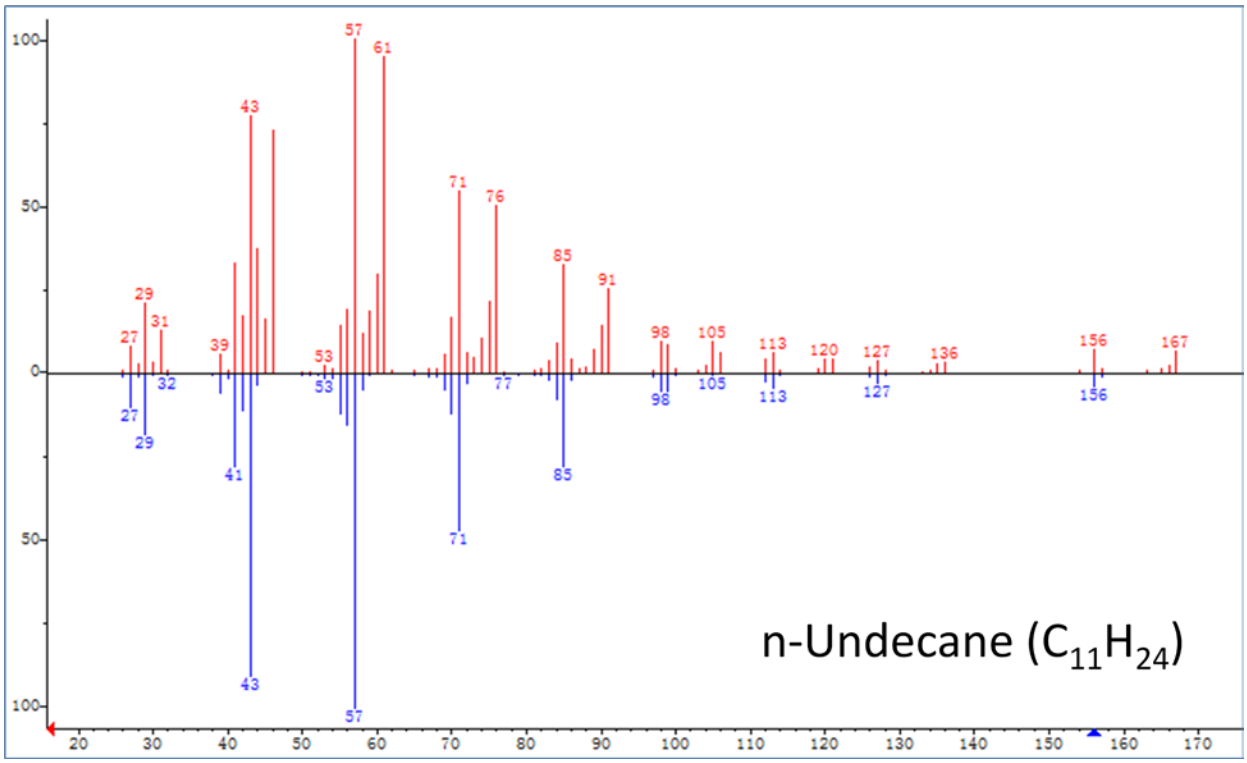
n-Undecane ($C_{11}H_{24}$)

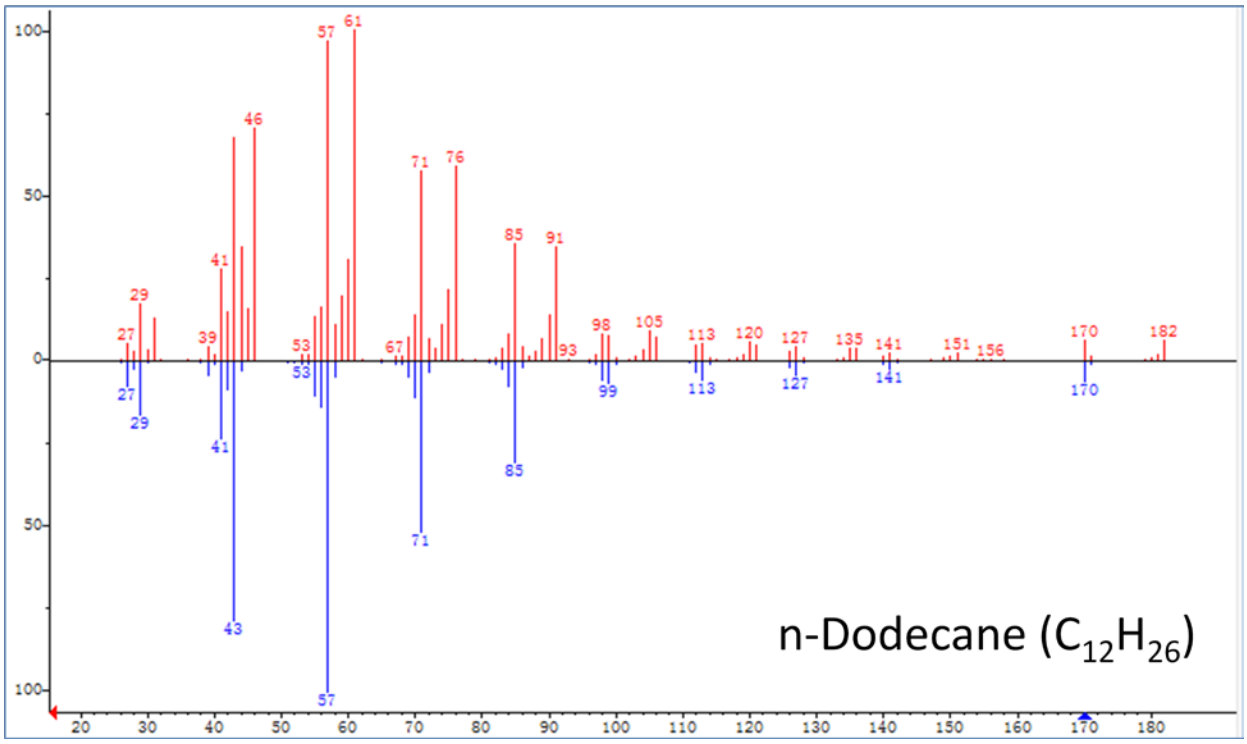
n-Dodecane ($C_{12}H_{26}$)

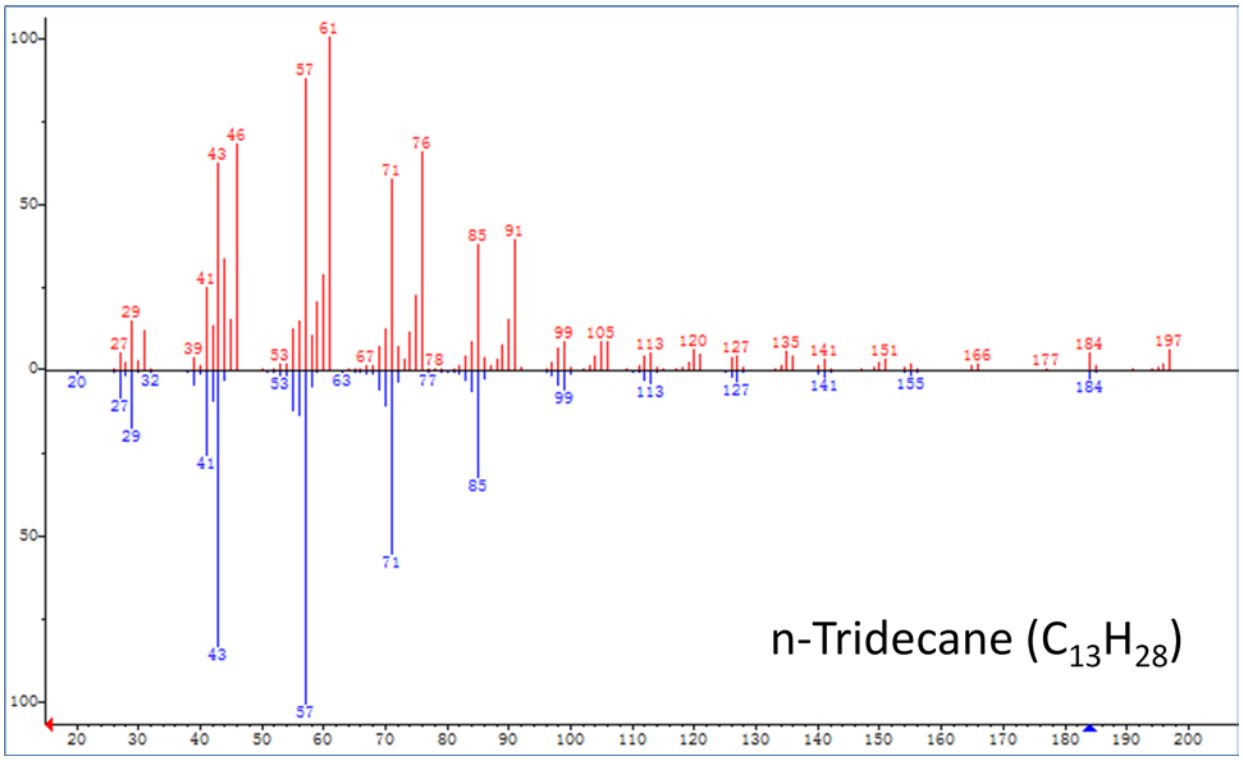
n-Tridecane ($C_{13}H_{28}$)

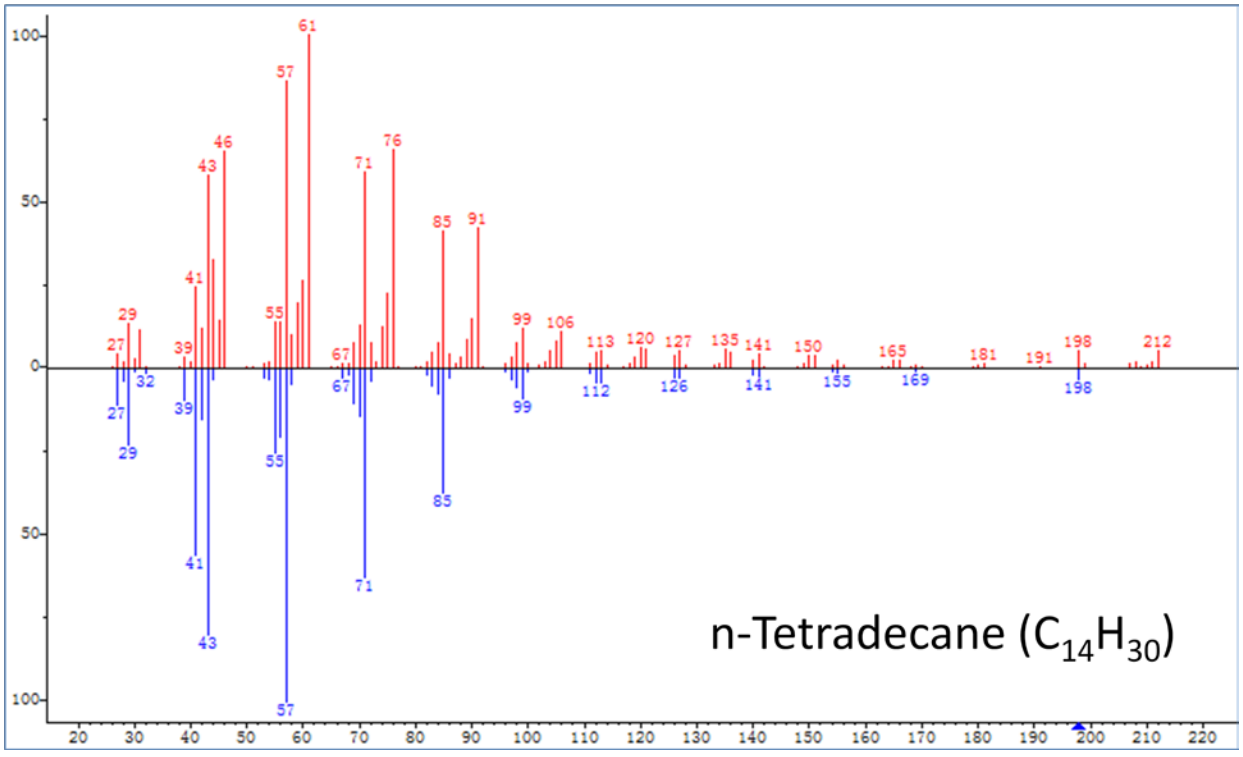
n-Tetradecane ($C_{14}H_{30}$)

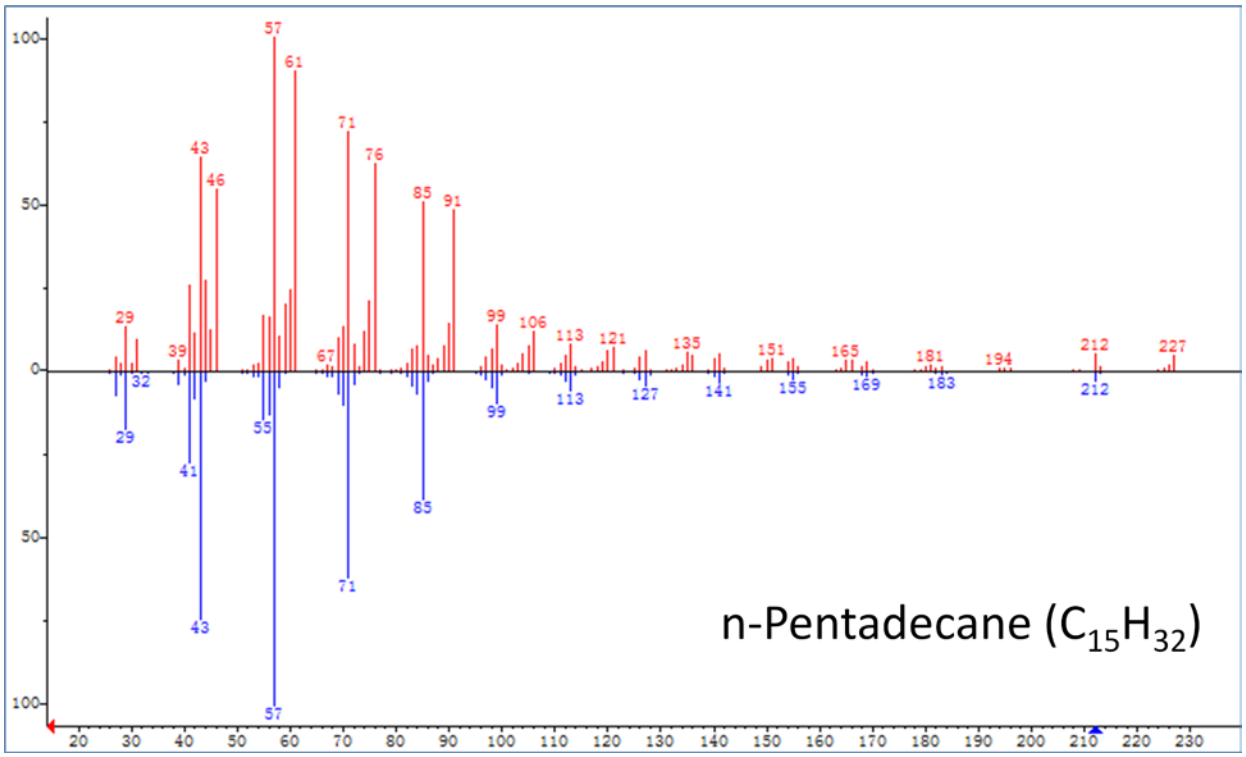
n-Pentadecane ($C_{15}H_{32}$)

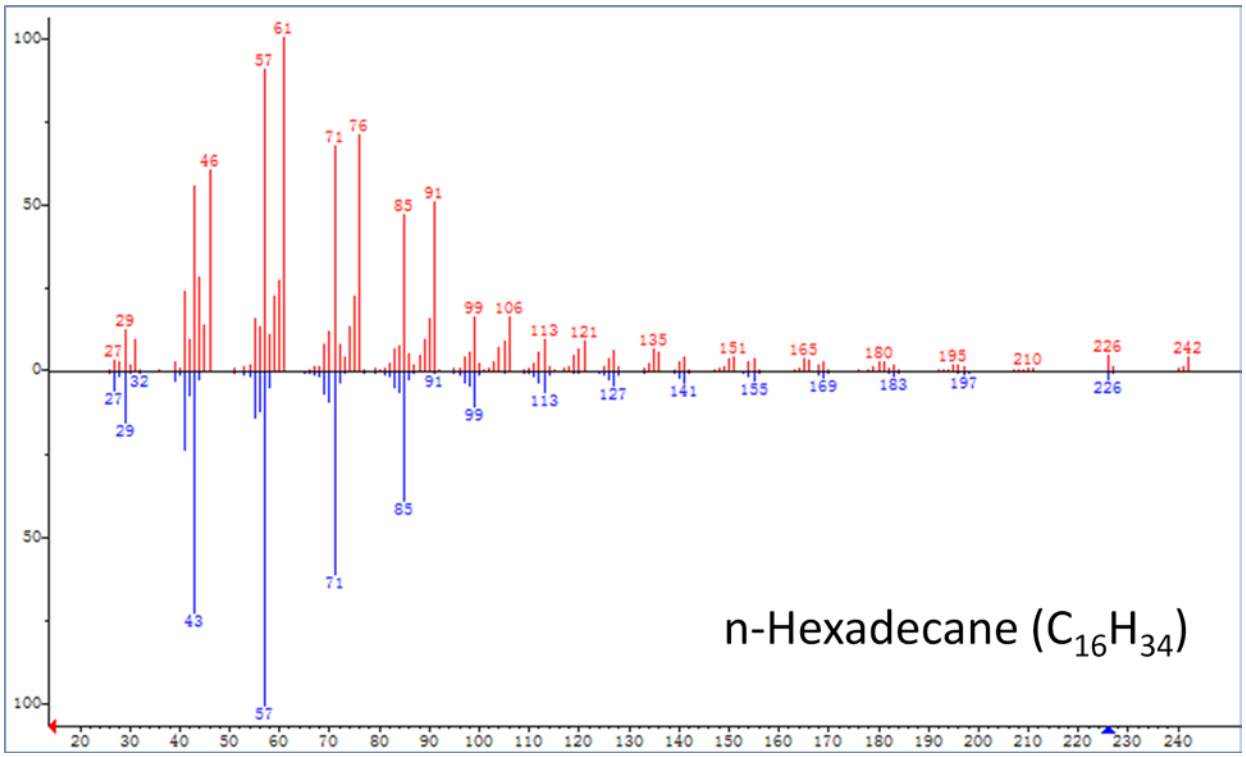
n-Hexadecane ($C_{16}H_{34}$)

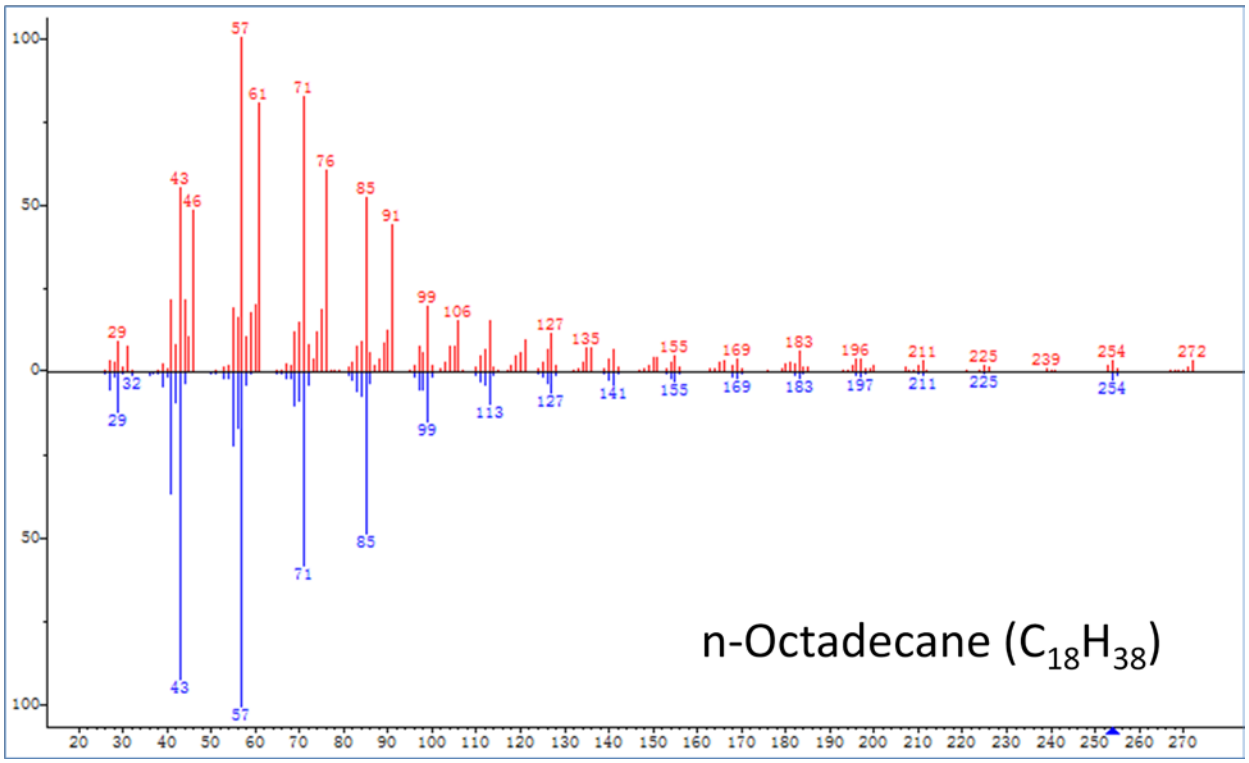

Fig. S12. GC-MS spectra of ^{13}CO labeling test. 0.2 MPa ^{13}CO, 3.8 MPa CO_2 and 4 MPa H_2 were used as reactant gases, and other conditions are the same as that of entry 1 in Table 1.

Note: We have marked several MS spectra of the paraffins (C4-C9) with green boxes, and all the spectra in this test had the similar rule. The pattern of MS signals inside and outside the green boxes are exactly the same as that of the standard spectra (blue lines), respectively. Moreover, the mass-to-charge ratio (m/z) of the signals inside each box is larger than that of the same pattern outside the box, and the difference in m/z is exactly equal to the carbon number in each fragment ion. Thus in each MS spectrum, the signals outside the green boxes belong to the paraffins from CO_2 because they agree well with the standard spectrum. Correspondingly, the signals in the green boxes are contributed by paraffins from ^{13}CO. If ^{13}C and C atoms coexisted in the same paraffin molecules generated in the reaction, the perfect rules in the current MS spectra discussed above will be destroyed. These results confirmed that ^{13}CO did not enter the chain growth of the paraffin produced from CO_2, and CO_2 did not take part in the chain growth of the paraffin generated from ^{13}CO either, as shown in the following equations. Thus, we can conclude that the hydrogenation of CO_2 to the paraffins did not proceed via CO.

$$^{13}CO + H_2 \xrightarrow{Co_6/MnO_x} {}^{13}CH_3(^{13}CH_2)_n{}^{13}CH_3 + H_2O$$

$$^{12}CO_2 + H_2 \xrightarrow{Co_6/MnO_x} {}^{12}CH_3(^{12}CH_2)_n{}^{12}CH_3 + H_2O$$

Table S1. The results of ICP-OES and XPS analysis of the Co-Mn bimetallic catalysts.

Catalyst	Co/Mn atomic ratio		
	Design value	Overall composition (ICP-OES)	Surface composition (XPS)
Co_2/MnO_x	2	2.01	1.9
Co_6/MnO_x	6	5.92	5.8
Co_{10}/MnO_x	10	9.89	9.1
Co_{14}/MnO_x	14	13.95	14.4

Table S2. Hydrogenation of other C1 resources.[*]

Entry	C1 source	Selectivity (C-mol%)			Activity ($mmol_{C1} \cdot g_{cat}^{-1} \cdot h^{-1}$)
		C_{1-4}	C_{5+}	ROH	
1[†]	CO	94.9	1.3	3.8	1.2
2[‡]	CO	84.3	9.1	6.6	3.1
3[#]	CH_3OH	88.7	11.3	-	4.2
4[#]	HCOOH	87.4	1.1	11.5	0.9

[*]Reaction conditions were the same as the entry 1 of Table 1, except CO_2 was replaced by other C_1 sources. [†]The CO pressure was 0.5 MPa. [‡]The CO pressure was 4 MPa. [#]The molar quantity of C1 source was equal to that of CO_2 in entry of Table 1.

Note: The alcohols (ROH) in CO hydrogenation were methanol and a small amount of ethanol, while only methanol was observed in hydrogenation of HCOOH.

Details of Materials and Methods

Chemicals. $Mn(NO_3)_2 \cdot 4H_2O$ (98.0%), Mn powder (99.6%), MnO powder (99%, 200 mesh), CoO (99.995%), Co_3O_4 (99.7%), cyclohexane (99.5%) were provided by Alfa Aesar. $Co(NO_3)_2 \cdot 6H_2O$ (≥99.0%) and MnO_2 (98%) were obtained from Sinopharm Chemical Reagent Co., Ltd. Squalane (99.0%) was provided by ACROS Organics. 1,3-Dimethyl-2-imidazolidinone (DMI, 99%) and benzene (99.5%) were purchased from TCI Shanghai Co, Ltd. $Al(NO_3)_3 \cdot 9H_2O$ (99.0%) was provided by Aladdin Industrial Corporation. $Ce(NO_3)_3 \cdot 6H_2O$ (>99.0%) was obtained from Tianjin Fuchen Chemical Reagents Factory. $Zn(NO_3)_2 \cdot 6H_2O$ (≥99.0%) was purchased from Guangdong Guanghua Sci-Tech Co., Ltd. CO_2 (99.99%), CO (99.99%) and H_2 (99.99%) were purchased from Beijing Analytical Instrument Company. ^{13}CO (^{13}C, 99%) was offered by Cambridge Isotope Laboratories, Inc., USA. All the chemicals were used without further pretreatments.

Catalyst characterization. The N_2 adsorption test was conducted on a Micromeritics ASAP 2460. The ICP-AES data was collected by an Agilent 5110 VDV ICP-OES. The XRD characterization was carried out on a Rigaku D/max 2500 with nickel filtered Cu-Kα operated at 40 kV and 20 mA. The XPS spectra were collected on an ESCALab 220I-XL electron spectrometer from VG Scientific using 300 W AlKα radiation. The binding energies were calibrated with the C1s level of adventitious carbon at 284.8 eV. The TEM characterization was conducted on a JEM-2100F electron microscope. The H_2-TPR test was performed on a chemisorption analyzer (Autochem 2950HP) from Micromeritics. Before test, the catalyst was heated at 300 ^oC for 30 min in 50 ml/min Ar. Then it was cooled to 50 ^oC and the gas flow was replaced by 30 ml/min 10%H_2-90%Ar. The data was collected from 50 ^oC to 750 ^oC at 10 ^oC/min. The TPD analysis also used the above apparatus. In CO_2-TPD test, the catalyst was heated to 100 ^oC in 50 ml/min He. After 1 h the temperature was reduced to 50 ^oC, and CO_2 adsorption began with 50 mL/min CO_2 for 1 h. Then the sample was purged with 50 ml/min He for 1 h, finally, CO_2 desorption proceeded from 50 to 600 ^oC at 10 ^oC/min. In H_2-TPD test, the catalyst was heated to 100 ^oC in 50 mL/min Ar. After 1 h the temperature decreased to 50 ^oC, and H_2 adsorption began with 50 mL/min 10%H_2-90%Ar for 1 h. Then the sample was purged with 50 mL/min Ar for 1 h, finally, the H_2 desorption proceeded from 50 to 600 ^oC at 10 ^oC/min.

Reference

1. Ahn, CI et al (2016) Water gas shift reaction on the Mn-modified ordered mesoporous Co_3O_4. Microporous Mesoporous Mater. 221: 204-211.
2. Kim KS (1975) X-ray-photoelectron spectroscopic studies of electronic-structure of CoO. *Phys Rev B* 11: 2177-2185.
3. Biesinger MC, et al. (2011) Resolving surface chemical states in XPS analysis of first row transition metals, oxides and hydroxides: Cr, Mn, Fe, Co and Ni. *Appl Surf Sci* 7: 2717-2730.
4. Wagner CD, Riggs WM, Davis LE, Moulder JF, Muilenberg GE (1979) Handbook of X-ray photoelectron spectroscopy (Perkin-Elmer Corporation, Minnesota).